Chinese Herbal Medicines 13 (2021) 381–388

Contents lists available at ScienceDirect

Chinese Herbal Medicines

journal homepage: www.elsevier.com/locate/chmed

Original Article

Polyphenols from *Securidaca inappendiculata* alleviated acute lung injury in rats by inhibiting oxidative stress sensitive pathways

Cong-lan Ji [a,1], Sheng Dai [a,1], Hong Liu [a], Ji-yang Dong [b], Chun-sheng Liu [c], Jian Zuo [c,d,e,*]

[a] *Department of Pharmacy, Anhui College of Traditional Chinese Medicine, Wuhu 241000, China*
[b] *Department of Electronic Science, Xiamen University, Xiamen 361005, China*
[c] *Yijishan Hospital, Wannan Medical College, Wuhu 241000, China*
[d] *Key Laboratory of Non-coding RNA Transformation Research of Anhui Higher Education Institution (Wannan Medical College), Wuhu 241000, China*
[e] *Provincial Engineering Laboratory for Screening and Re-evaluation of Active Compounds of Herbal Medicines in Southern Anhui (Wannan Medical College), Wuhu 241000, China*

ARTICLE INFO

Article history:
Received 31 July 2020
Revised 15 September 2020
Accepted 25 September 2020
Available online 2 March 2021

Keywords:
antioxidant
polyphenols
reactive oxygen species (ROS)
Securidaca inappendiculata Hassk
TLR4/NF-κB

ABSTRACT

Objective: *Securidaca inappendiculata* is a medicinal plant frequently used in the treatment of inflammatory diseases in south China. In this study, we aimed to explore its bioactive constituent which contributes to the anti-inflammatory activity.

Methods: Polyphenol-enriched and polyphenol-deprived fractions (PRF and PDF, respectively) were separated from the ethanolic extract by HPD300 macroporous resin-based method, and their anti-inflammatory activities were investigated on a lipopolysaccharide (LPS)-induced acute lung injury (ALI) model in rats. The possible mechanism of action in alleviating acute inflammation was studied using RAW264.7 cells.

Results: Both Folin-Ciocalteu and ^{1}H nuclear magnetic resonance (NMR) analyses showed that polyphenolic content in PRF was approximately 10 times higher than that of PDF, and this observation reflected in their antioxidative capacities. PRF but not PDF significantly decreased the level of malondialdehyde, suppressed the expression of nicotinamide phosphoribosyltransferase (NAMPT) protein, and improved the severity of ALI in rats. PRF at 10 μg/mL effectively downregulated the expression of proteins NAMPT, HMGB1, TLR4, and p-p65, and scavenged the intracellular reactive oxygen species (ROS) in LPS-primed RAW264.7 cells. *N*-acetyl-*L*-cysteine exhibited similar inhibitory effects on ROS production and NAMPT-mediated TLR4/NF-κB activation *in vitro*, whereas nicotinamide mononucleotide antagonized all the changes induced by PRF during cotreatments.

Conclusion: As an antioxidant, PRF exhibited potent anti-inflammatory activity under both *in vivo* and *in vitro* conditions by downregulating NAMPT and TLR4/NF-κB. Accordingly, polyphenols were identified as important bioactive constituents in *S. inappendiculata* targeting oxidative stress-sensitive pro-inflammatory pathways.

1. Introduction

Securidaca inappendiculata Hassk. is a plant that belongs to the genus *Securidaca* Linn and is native to south China. The plant is traditionally used in the treatment of inflammations and rheumatoid arthritis. Previous studies have explored the anti-inflammatory, antitumor, and hepatoprotective activities of *S. inappendiculata* (Li, 2005; Yang, 2001). Some studies have shown the presence of xanthones, terpenoids, polyphenols, steroids, and lignans in *S. inappendiculata* (Yang, 2001; Ji, Wang, Wang, Chen, & Li, 2019; Zuo, Mao, Yuan, Li, & Chen, 2014a). Aside from fatty acids, lipophilic fraction of *S. inappendiculata* is rich in xanthone derivatives that demonstrate significant anti-inflammatory activity both *in vivo* and *in vitro* (Zuo, Xia, Mao, Li, & Chen, 2014b; Zuo, Xia, Li, & Chen, 2014c, 2014d; Jiang, Ji, Yang, Zhang, & Zuo, 2018). Although xanthones exhibit potent therapeutic efficacy in inflammatory diseases, their distribution is limited (Yang, 2001; Zuo et al., 2014a).

α-Mangostin (a prenylated xanthone isolated from mangosteen) has shown inhibitory effects against nicotinamide phosphoribosyltransferase (NAMPT) signaling, thereby reducing inflammatory reactions (Tao et al., 2018). Of note, this compound exerted significant therapeutic effects on acute lung injury (ALI)

* Corresponding author.
E-mail address: zuojian8178@163.com (J. Zuo).
[1] These authors contributed equally to this work.

https://doi.org/10.1016/j.chmed.2020.09.007
1674-6384/

in vivo, which is usually induced with LPS in rodent, and extensively used as an acute inflammation model (Tao et al., 2018; Yang et al., 2020). Considering the difficulties in effectively controlling acute inflammations, this medicinal property of α-mangostin as well as relevant chemicals are especially meaningful. Since NAMPT is an indispensable component in the free radical scavenging system, it is usually upregulated by the presence of reactive oxygen species (ROS) (Cerna et al., 2012). Accordingly, antioxidant properties of certain polyphenols are theoretically beneficial for the alleviation of NAMPT-mediated inflammation. We hypothesized that polyphenols sharing certain structural and chemical similarities with xanthones are capable of controlling NAMPT signaling. To verify above hypothesis, we tested effects of *S. inappendiculata*-derived polyphenols on ALI in this study, and clarified its relevance to NAMPT signaling changes.

2. Materials and methods

2.1. Chemicals and reagents

Folin-Ciocalteu reagent (FCR) and tripyridyltriazine (TPTZ) were purchased from Solarbio Science and Technology Co., Ltd. (Beijing, China). The following chemicals were obtained from KeyGen Biotech (Nanjing, China): 2, 2-diphenyl-1-picryl-hydrazyl (DPPH); 3-[4, 5-dimethylthiazol-2-yl]-2, 5 diphenyl tetrazolium bromide (MTT); 2′, 7′-dichlorodihydrofluorescein diacetate (DCFH-DA); lipopolysaccharide (LPS, from *Escherichia coli* O111:B4); phosphate-buffered saline (PBS); *N*-acetyl-*L*-cysteine (NAC); BCA protein quantitative kit; and nicotinamide mononucleotide (NMN). Fetal bovine serum (FBS), high-glucose Dulbecco's modified Eagle's medium (DMEM), enhanced chemiluminescence (ECL) detection kit, and bovine serum albumin (BSA) were obtained from Thermo Scientific (Rockford, IL, USA). The primary and secondary antibodies were obtained from Affinity Biosciences (Cincinnati, OH, USA). All other chemicals and solvents were of analytical grade and obtained from Guanghua Sci-tech (Shantou, China).

2.2. Extraction and separation of fractions

The crude drug was identified as the bark of *S. inappendiculata* by associate Professor Jian Zuo (Wannan Medical College, Wuhu, China). Voucher specimen (ID: 2017-11-034) has been deposited at the Herbarium Institution in Anhui College of Traditional Chinese Medicine. The bark was refluxed twice with 95% ethanol and the filtrate was combined. The combined filtrate was evaporated under reduced pressure with a rotatory evaporator. This dried crude extract was then dissolved with distilled water and subjected to separation on an HPD300 macroporous resin column. A gradient mixture of EtOH/H_2O (5%–95%) was used to elute the components. The eluate was collected as two parts: part A was eluted with ≤15% ethanol and part B was eluted with >15% ethanol. Part B was evaporated and the dried residue was dissolved in 0.5% sodium hydroxide solution. The undissolved portion combined with part A was taken as polyphenol-deprived fraction (PDF). The solution was then acidified with hydrochloric acid and the obtained precipitate was designated as polyphenol-enriched fraction (PRF). The yields of PDF and PRF were 9.9% and 2.0%, respectively.

2.3. Determination of polyphenolic content and antioxidant activity

Samples (dissolved in 40% ethanol), methanol, and FCR were mixed in equal volumes (0.5 mL for each) and allowed to stand for 3 min. Then, 1 mL of 20% sodium carbonate solution was added and incubated for 30 min in the dark. Then, the optical density (OD) of the reaction mixture was read at 760 nm on a Cary 60 UV–Vis spectrophotometer (Agilent Technologies, Santa Clara, USA). Concentrations of polyphenols were calculated with a calibration curve prepared by using gallic acid as the reference compound. Another portion of samples were dissolved in dimethyl sulfoxide (DMSO) and subjected to ^{1}H nuclear magnetic resonance (NMR) analysis using a 600 MHz Varian Inova spectrometer (Agilent Technologies, Palo Alto, USA). Chemical shifts within the range of 6–8 × 10^{-6} were regarded as characteristic signals of aromatic protons and the relative intensities were used to assess the distribution of polyphenols in mixtures.

Next, 100 μL of sample and DPPH solution were thoroughly mixed and incubated for 30 min. Then, the absorbance was read at 517 nm (A). The absorption of control and blank DPPH solutions was simultaneously read as B and C. Antioxidant capacity was assessed based on the following equation:

$$\text{Scavenging rate}(\%) = (1 - (A - B)/C) \times 100$$

Aqueous solution of $FeCl_3 6H_2O$, TPTZ solution, and sodium acetate-acetic acid buffer were mixed at the ratio of 1:1:10. The mixture (150 μL) and samples (20 μL) were incubated at 37 °C for 10 min and then the absorbance was read. The absorption of a series of standard Fe^{2+}-TPTZ solution was determined beforehand and the antioxidant capacity of samples were normalized to the production of Fe^{2+}.

2.4. High-pressure liquid chromatographic (HPLC) analysis

Qualitative analyses of PRF and PDF were performed on a Waters 1525 HPLC system coupled with a 2487 UV detector (Waters, Milford, MA, USA) by using a XBridge C_{18} column (3.5 μm, 4.6 × 150 mm, Waters, Dublin, Ireland). A gradient elution at the flow rate of 1 mL/min was adopted. Methanol and water were used as the mobile phase B and A, respectively. The elution program was as follows: 0–30 min, B 30%–60%; 30–40 min, B maintained at 60%. The column temperature and detection wavelength were set at 25 °C and 264 nm, respectively. The data were acquired and processed by Breeze software, version 3.30 (Waters, Milford, MA, USA).

2.5. Induction of ALI in rats

Male Sprague Dawley rats (7 weeks old) were obtained from Qinglongshan Laboratory Animal Company, Nanjing, Jiangsu, China, which were housed under controlled conditions [(21 ± 1) °C, (50 ± 5)% relative humidity] with a 12 h light and 12 h dark cycle. After the acclimatization period, the rats were randomly assigned to six groups with six rats per group as follows: group 1, healthy control rats; group 2, ALI model rats; group 3, low-dose PDF-treated rats (40 mg/kg); group 4, high-dose PDF-treated rats (120 mg/kg); group 5, low-dose PRF-treated rats (40 mg/kg); group 6, high-dose PRF-treated rats (120 mg/kg). Treatment groups were administered with PDF or PRF by oral gavage for three consecutive days, whereas normal and ALI model rats were administered with 0.5% CMC-Na. After 3 d of treatments, all rats, except the normal controls, were challenged by LPS to induce ALI according to the procedures reported previously (Agorreta, Zulueta, Montuenga, & Garayoa, 2005). Briefly, LPS was dissolved in saline at the concentration of 5 mg/mL. All the ALI rats received a single dose of LPS injection at 5 mg/kg intraperitoneally. After 12 h, significant manifestations of ALI were developed in LPS-treated rats, including respiratory distress, foam-like discharge from nose, and reduced response to stimuli. All animal experiments were performed in accordance with the guidelines of Institutional Animal Care and Use Committee of Wannan Medical College (Ethics Approval Number: YJS 2017-11-021).

2.6. Sacrifice and tissue sampling

At the end of the experiment, rats were anesthetized with 10% chloral hydrate solution, and their blood samples were obtained through abdominal aorta. One portion of the blood sample was collected in anticoagulation tubes for full blood count (FBC) analysis with the aid of an automated hematology system (ADVIA 120, Bayer Diagnostics, German). Another portion of blood was collected into promoting coagulating tubes to separate serum, which was used for the determination of malondialdehyde (MDA), tumor necrosis factor (TNF)-α and extracellular NAMPT (eNAMPT) by using quantification kits (JianCheng Bioengineering Institute, Jiangsu, China). The lungs were dissected immediately, washed with cold PBS and fixed in neutral buffered formalin.

2.7. Histological and immunohistochemical examinations

The fixed lung tissue samples were cut and washed with running tap water. After dehydration with ethanol, the specimens were cleared with xylene, embedded in paraffin, and sectioned. The sections were subsequently deparaffinized and stained with hematoxylin/eosin (H&E). The severity of ALI was assessed based on the observation under BH-2 microscope (Olympus, Tokyo, Japan) for typical pathological changes such as alveolar edema or alveolar wall thickening, alveolar hemorrhage, and neutrophil infiltration. Certain dewaxed lung sections were used for immunohistochemical analysis. After deactivation of endogenous peroxidase, the epitope was retrieved using citric acid incubation method. The sections were then incubated with normal goat serum, specific primary antibody, and horseradish peroxidase (HRP)-conjugated secondary antibody in turns. The targeted proteins were visualized by staining with 3,3-diaminobenzidine and counterstained with hematoxylin.

2.8. Prussian blue staining and immunoblotting

ALI is typically defined as a neutrophil-mediated disease. However, convincing evidence suggests that macrophages play an indispensable role in the onset and development of ALI by recruiting neutrophil and initiating cytokines storm (Soni et al., 2016). Being a classic agonist of the pattern recognition receptor TLR4, LPS elicits acute and severe inflammatory reactions in ALI rats mainly by activating macrophages (Dong, Wang, Chen, Li, & Bi, 2008). Thereby, a mice macrophage-derived RAW264.7 cell line was adopted in this study *in vitro*, which was grown in high-glucose DMEM supplemented with 10% FBS under routine culture conditions (37 °C, 5% CO_2). The cells were passaged every 2 d at the ratio of 1:3. Cells were seeded into 24-well plates and allowed for attachment overnight. After PRF treatment, the cells were stained with Prussian blue. The cells stained with blue were deemed as dead. Cytotoxicity of PRF was evaluated based on the percentage of dead cells.

Cells seeded into 6-well plates were pretreated by LPS. After 1 h, PDF/PRF (or together with NAC/NMN) was added. The cells were harvested and lysed with cold RIPA buffer. The supernatant of the lysate was spiked into loading buffer and denatured by boiling. Samples containing equal amount of proteins were subjected to sodium dodecyl sulfate–polyacrylamide gel electrophoresis (SDS-PAGE) and the separated proteins were subsequently transferred onto polyvinylidene fluoride (PVDF) membranes. Later, the membranes were then treated with 5% BSA, primary and HRP-tagged secondary antibodies. The signals were developed and detected using an ECL kit on a ChemiDoc XRS$^+$ system (Bio-Rad Laboratories Inc., USA).

2.9. Intracellular ROS assessment

Cells were seeded in 6-well plates and pretreated with LPS for 1 h, followed by PRF treatment (or in combination with NMN). Subsequently, the supernatant was replaced by fresh DCFH-DA-containing serum-free medium. After incubation, excessive probe was washed and the fluorescence was observed using a BX53 fluorescence microscope (Olympus, Tokyo, Japan). The intracellular levels of ROS were analyzed with the aid of flow cytometry (FACS Calibur system, Becton and Dickson, San Jose, CA, USA).

2.10. Statistical analysis

Data were expressed as mean ± standard deviation (SD). Statistical differences among groups were compared using one-way ANOVA and post hoc test with the aid of SPSS software, version 14.0 (SPSS Inc. Chicago, IL, USA).

3. Results

3.1. Chemical profile and antioxidant capacity of PDF and PRF

FCR quantitative assay showed that total contents of polyphenols in PDF and PRF were 1.53% and 12.69%, respectively. To confirm this, polyphenol distribution was further assessed with a ^{1}H NMR-based strategy. It was observed that aromatic protons contributed 0.44% and 5.51% to the total signal intensity in PDF and PRF, respectively (Fig. 1A), which was consistent with the results obtained from FCR assay. HPLC analyses confirmed the difference in chemical composition between PRF and PDF. The chromatograms showed that hydrophilic constituents of PRF and PDF shared similar profiles, whereas most of the lipophilic compounds with intense optical absorption at 264 nm were not detected in PDF (Fig. 1B). By comparing with reference compounds isolated previously, it was found that 1,7-dihydroxy-3,4-dimethoxyxanthone was the dominant in PRF. Both ferric ion reducing antioxidant power (FRAP) and DPPH assay indicated that PRF possessed more powerful antioxidant capacity than PDF (Fig. 1C). Although the efficiency was not strictly proportionate to the polyphenol content, there was an obvious correlation between them, especially at low concentrations. DPPH analysis revealed that PRF at 0.3125 mg/mL scavenged 68.32% of the free radicals, whereas PDF at the same concentration only reduced 7.70% of the DPPH radicals. Similar results were obtained in the case of FRAP assay.

3.2. PRF treatments reduced severity of ALI in rats

Extensive inflammatory infiltration and alveolar hemorrhage were readily noticed in ALI rats. LPS challenge also induced significant alveolar edema. PDF treatment slightly alleviated the severity of ALI, whereas the pathological changes were still vividly obvious even in the high-dose group. While PRF exhibited superior therapeutic effects at 120 mg/kg, all abnormal changes were efficiently suppressed (Fig. 2A). FBC analysis found that LPS challenge greatly affected monocyte distribution. Its population was increased by approximately 4-fold in ALI rats, which was then completely restored by PRF but not PDF. This change resulted in a decrease in the white blood cell count in PRF-treated group (Fig. 2B). In addition, LPS-induced increase in the levels of MDA and TNF-α was significantly suppressed by PRF treatment, whereas PDF treatment showed no significant effects when compared with ALI model group (Fig. 2C). Reduced levels of MDA not only indicated the eased oxidative stress under *in vivo* conditions but also served as an indicator of restored lipid metabolism (Tsikas, 2016). By taking the central metabolic role of nicoti-

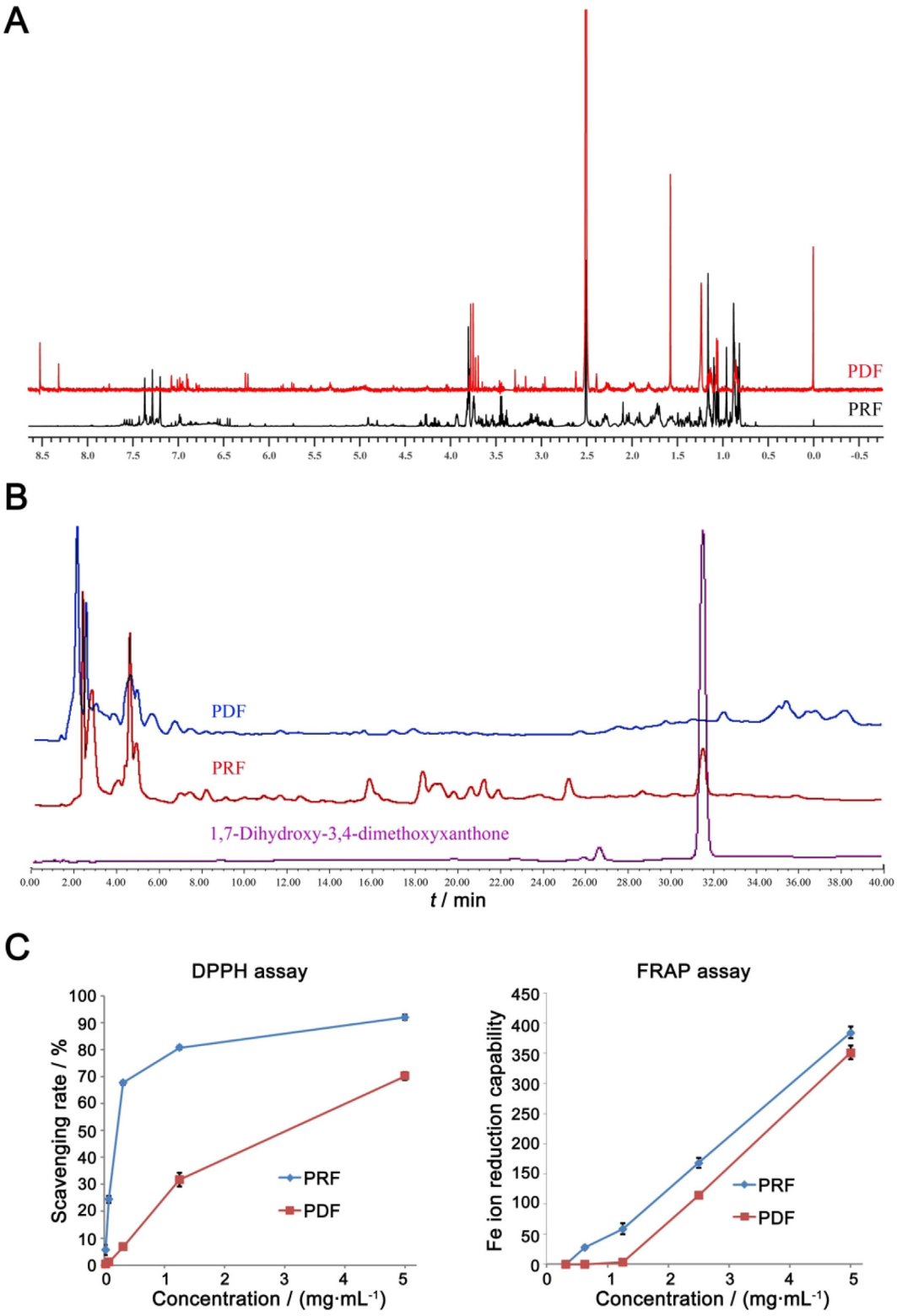

Fig. 1. Different chemical profiles between PRF and PDF. A, ^{1}H NMR spectrums of two fractions; B, Representative HPLC chromatograms of PRF, PDF and reference compound; C, Varied anti-oxidative capacities of PRF and PDF revealed by DPPH and FRAP assays.

namide adenine dinucleotide (NAD) into consideration, we could partially link the negative effect of PRF on the production of MDA production to its inhibition on NAMPT. Consistent to this hypothesis, reduced levels of eNAMPT were observed under PRF treatments (Fig. 2C).

3.3. PRF suppressed expression of NAMPT protein

As increased NAMPT is favorable for M1 polarization of monocyte/macrophage and thereby promotes the development of inflammation, it was not surprised to find that its expression was

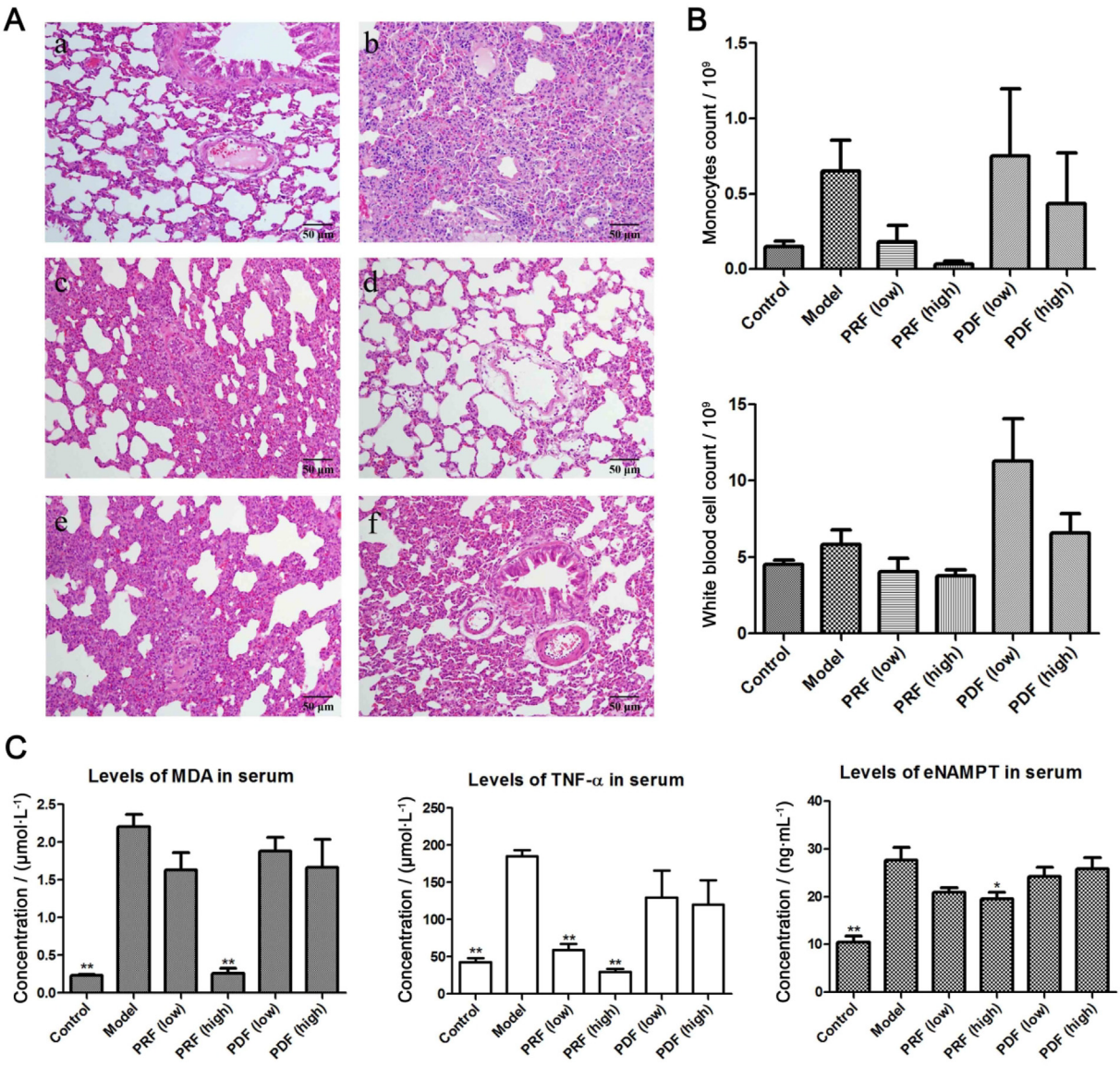

Fig. 2. Therapeutic effects of PRF and PDF on ALI rats. A, Histological examination of lung tissue: a-f represent normal, ALI model, PRF (low dose), PRF (high dose), PDF (low dose), PDF (high dose) groups, respectively; B, Results of FBC analysis; C, Levels of inflammatory biomarkers in serum. Data represent as mean ± SD, n = 6. Statistical significance: $^{*}P < 0.05$ and $^{**}P < 0.01$ compared with model control.

greatly upregulated in ALI rats. Treatments of PRF and PDF led to varied outcomes. NAMPT expression in ALI rats was effectively suppressed by PRF in a dose-dependent manner, while PDF barely affected it (Fig. 3A). Of note, level of NAMPT in ALI rats was reduced by PRF at 120 mg/kg to the extent even lower than that in normal healthy controls. Subsequently, we attempted to verify this observation *in vitro*. In order to mimic the inflammatory conditions *in vivo*, we pretreated RAW264.7 cells with LPS, which resulted in the upregulation of NAMPT. PRF treatments exhibited similar inhibitory effects on NAMPT protein expression *in vitro*. However, according to our observation, treatment with high concentrations of PRF yielded poor efficacy (Fig. 3B). That is, PRF effectively suppressed NAMPT expression at 10 and 20 μg/mL, while no obvious change was observed when the treatment concentration was increased to 30 μg/mL. PDF treatment had no effect on the levels of NAMPT in LPS-primed RAW264.7 cells.

3.4. Effects of PRF on NAMPT were mediated by intracellular ROS

As NAMPT serves as an important survival signaling molecule, the abnormal upregulation of NAMPT under increased exposure to PRF might be triggered by increased rate of apoptosis (Yang et al., 2019). In this study, the cells were manually counted with the help of Prussian blue staining. Overall cell counts were not dramatically decreased after PRF treatment, but dead cells were significantly increased by the increase of treatment concentrations. PRF inhibited NAMPT protein expression initially, but the trend was reverted at concentrations of 30 and 50 μg/mL, which was consistent to our hypothesis (Fig. 4A).

Higher concentration of polyphenol stimulates ROS production and eventually leads to apoptosis. The inconsistent effects of PRF on NAMPT signaling could be mediated by ROS accumulation. As expected, PRF treatment increased the intracellular level of ROS

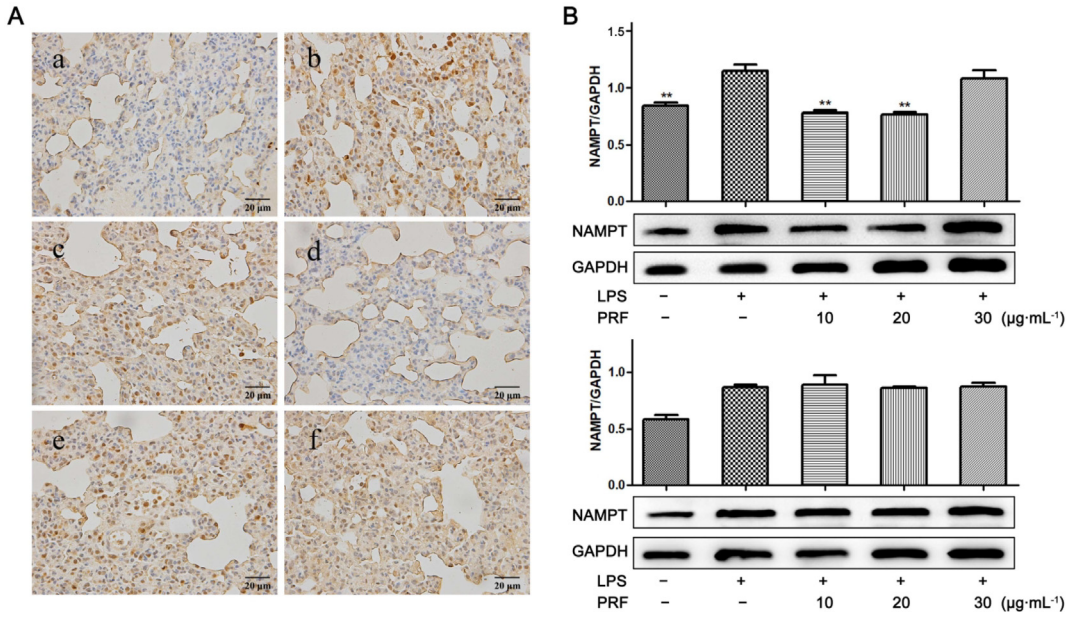

Fig. 3. Regulatory effects of PRF and PDF on NAMPT protein expression. A, Expression of NAMPT in lungs: a-f represent normal, ALI model, PRF (low dose), PRF (high dose), PDF (low dose), PDF (high dose) groups, respectively; B, Effects of PRF and PDF on LPS-elicited increases of NAMPT in RAW264.7 cells. Data represent as mean ± SD, $n = 6$. Statistical significance: $P^{*} < 0.05$ and $P^{**} < 0.01$ compared with LPS-treated cells.

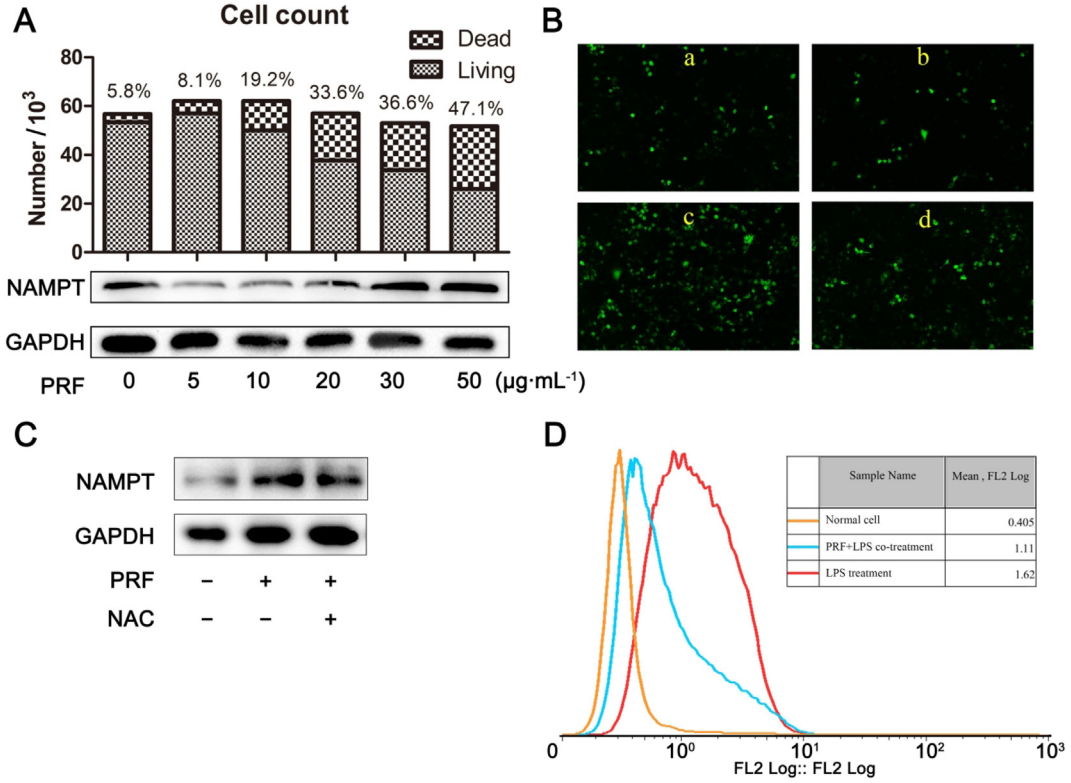

Fig. 4. Effects of PRF treatments on NAMPT expression and intracellular ROS in RAW264.7 cells. A, Correlation between cell viability and NAMPT expressions under PRF treatments; B, Intracellular ROS levels in cells receiving PRF treatments: a–c represent PRF-treated cells at 0, 10 and 40 μg/mL respectively, d represents PRF (40 μg/mL) + NMN cotreated cells; C, NAC suppressed NAMPT expression increase induced by intense PRF treatment (40 μg/mL); D, PRF (10 μg/mL) reduced LPS-induced intracellular ROS accumulation.

in a dose-dependent manner, whereas NMN (the biosynthesis precursor of NAD) significantly decreased oxidative stress (Fig. 4B). Collectively, it showed that ROS accumulation would upregulate NAMPT/NAD, whereas increased NAD might scavenge intracellular ROS. This self-balancing feedback was further validated, as intense PRF treatment-induced upregulation of NAMPT (40 μg/mL) was largely abrogated by NAC (Fig. 4C). Consequently, it was speculated that inhibition of low-dose PRF treatment on NAMPT under inflam-

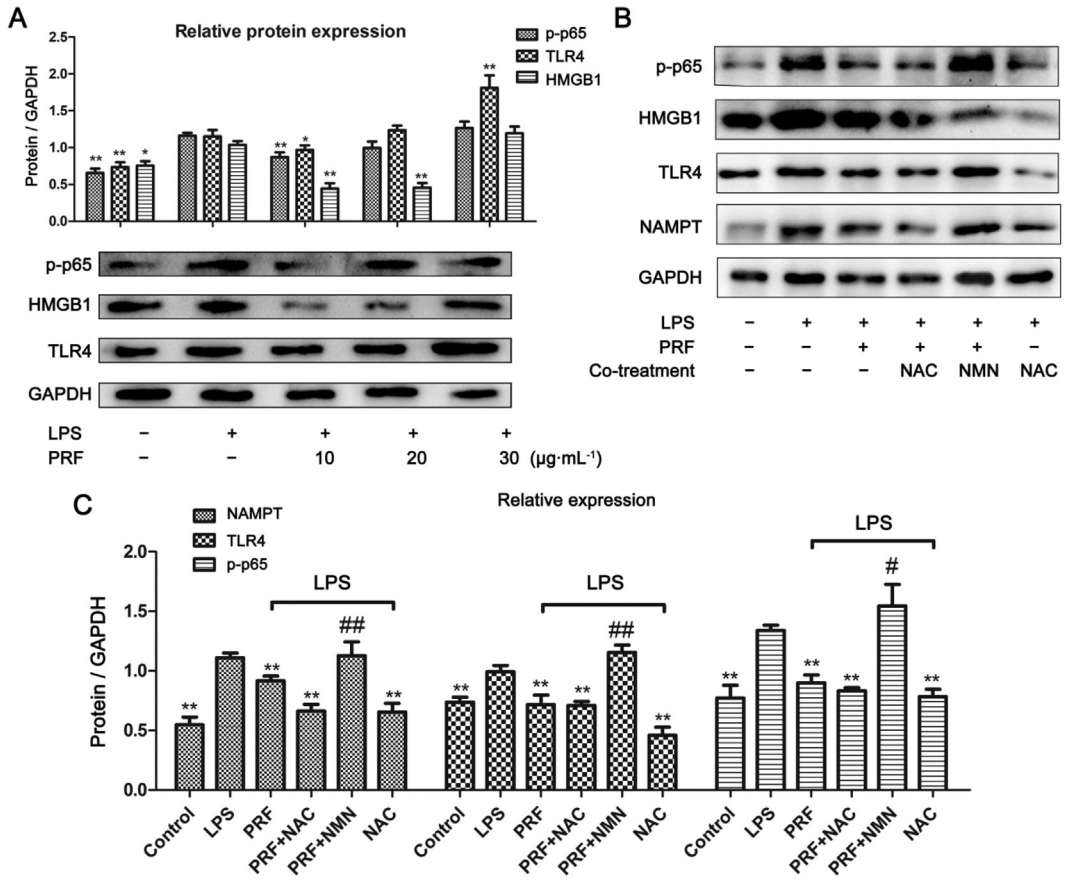

Fig. 5. Effects of PRF on NAMPT and TLR4/NF-κB pathway in RAW 264.7 cells *in vitro*. A, Effects of PRF on expression of proteins TLR4, HMGB1, and p-p65; B, Effects of NAC/NMN cotreatments on PRF-induced inhibition on NAMPT and TLR4/NF-κB; C, Quantified results of experiment B. Data represent as mean ± SD, $n = 6$. Statistical significance: $^{*}P < 0.05$ and $^{**}P < 0.01$ compared with LPS-treated cells, $^{\#}P < 0.05$ and $^{\#\#}P < 0.01$ compared with LPS + PRF treated cells.

matory conditions could be the result from reduced oxidative stress. Consistent to this notion, PRF at 10 μg/mL significantly reduced LPS-induced ROS accumulation (Fig. 4D). These data suggested that NAMPT signaling was highly stress-sensitive and fluctuates in accordance with the levels of ROS after PRF treatment.

3.5. NAMPT inhibition by PRF contributed to alleviated inflammation

As inflammation induced by LPS is a typical TLR4/NF-κB driven event, we subsequently investigated the hallmark proteins from this pathway. HMGB1 is well recognized as an important endogenous agonist for TLRs, and usually used as an indicator of TLR4 pathway status (Yu et al., 2006). Thereby, levels of p-p65, TLR4 as well as HMGB1 were investigated in this study. Consistent to its effects on NAMPT, PRF significantly suppressed the expression of proteins p-p65 and HMGB1 at low but not at high concentration (Fig. 5A). Furthermore, PRF at 10 μg/mL reduced the expression of NAMPT and TLR4 in LPS-primed cells. NAC stimulus exerted similar but even stronger effects on RAW264.7 cells compared with PRF and it largely overshadowed the effects of PRF in the cotreatment (Fig. 5B). Since NMN can substantially promote the expression of NAMPT, we managed to decipher the correlation between NAMPT levels and inflammation by cotreatment with NMN and PRF, and found that NMN-induced NAMPT upregulation greatly offset the inhibitory effect of PRF on TLR4/NF-κB signaling pathway (Fig. 5C). These clues further validated the therapeutic mechanisms of PRF on NAMPT-mediated inflammation by scavenging intracellular ROS.

4. Discussion

Literature is abundant on the anti-inflammatory properties of polyphenols. In this study, we further elucidated the anti-inflammatory mechanisms of *S. inappendiculate*-derived polyphenols involving the manipulation of oxidative stress. Previous studies have reported that xanthones are important bioactive components that can inhibit NAMPT signaling and subsequently cripple TLR4/NF-κB pathway (Tao et al., 2018; Yang et al., 2019; Zuo et al., 2017; Ji et al., 2017). Considering the structural similarities of some coexisting polyphenols from this plant with xanthone, it was hypothesized that these compounds could inhibit TLR4/NF-κB activation through a similar mechanism.

In this study, PRF treatment substantially suppressed NAMPT signaling under both *in vivo* and *in vitro* conditions. Although the clinical implication of overexpression of NAMPT is not fully understood, the pro-inflammatory role of its extracellular form (eNAMPT) has been firmly validated. It acts as a cytokine and elicits the process of activation of inflammatory pathways through interactions with TLR4 (Pulla et al., 2015; Camp et al., 2015). Furthermore, NAMPT can accelerate lipid metabolism by controlling Sirt1, which results in the accumulation of free fatty acids. Since fatty acids have been identified as TLR4 agonists, these changes will eventually lead to deteriorated inflammation (Hwang, Kim, & Lee, 2016). Therefore, NAMPT might be an ideal therapeutic target for TLR4-controlled inflammatory reactions (Pulla et al., 2015), and downregulation of NAMPT by PRF could at least be partially involved in therapeutic actions of *S. inappendiculata* on both acute inflammation and chronic arthritis. Because of their redox proper-

ties, many studies emphasize the effect of polyphenols on some oxidative stress-activated pathways such as NF-κB. This study further demonstrates that NAMPT is likewise a ROS-sensitive signaling pathway and inspires us to explore the anti-inflammatory mechanisms of antioxidants from a broader perspective.

Another interesting finding is the subtle effect of PRF on ROS levels. Although the ROS scavenging capacity of polyphenols has been confirmed by numerous researches, increasing evidences have demonstrated that they can also induce ROS accumulation, thus promoting apoptosis (Zhang et al., 2017; Ryu, Lim, Bazer, & Song, 2017). The exact dosage may serve as an important variable in deciding the final outcome. Consistent to this notion, at low concentrations, 1,7-dihydroxyl-3,4-dimethoxyl-xanthone efficiently inhibited NF-κB pathway. However, its anti-inflammatory effect was reduced at higher concentration, which was accompanied with accelerated ROS generation (Zuo et al., 2017). Similar phenomenon was observed in this study. Such a paradox reflects the complicated mechanism involved in the therapeutic action of polyphenols on inflammatory reactions and their dual effects on oxidative stress. However, the mechanism by which accumulated exposure of certain polyphenols such as xanthones promote ROS formation in cells is yet to be understood. More emphasis should be attached to this issue in future researches, as it is essential for fully understanding the effect of polyphenols on redox/oxidative balance and optimizing relevant therapeutic regimens.

5. Conclusion

This study has further identified that polyphenols are an important anti-inflammatory constituent in *S. inappendiculata*. By acting as an antioxidant, PRF eased oxidative stress and consequently inhibited NAMPT-mediated TLR4/NF-κB activation. Our results suggest that NAMPT is an important therapeutic target of polyphenols, and their antioxidant capacity is essential in controlling ROS-sensitive pro-inflammatory pathways.

Declaration of Competing Interest

The authors declare that they have no known competing financial interests or personal relationships that could have appeared to influence the work reported in this paper.

Acknowledgements

The authors thank Dr. Opeyemi Joshua Olatunji for polishing the language.

This work was supported by National Natural Science Foundation of China (81603388, 81973828 and 81173596), Major Project of Natural Science Foundation of the Department of Education of Anhui province (KJ2019ZD32), Funding of "Peak" Training Program for Scientific Research of Yijishan Hospital, Wannan Medical College (GF2019J01) and Key Project of Natural Science Foundation of Anhui Province for College Scholar (KJ2019A0416 and KJ2018A0249).

References

Agorreta, J., Zulueta, J. J., Montuenga, L. M., & Garayoa, M. (2005). Adrenomedullin expression in a rat model of acute lung injury induced by hypoxia and LPS. *American Journal of Physiology-Lung Cellular and Molecular Physiology, 288*, L536–L545.

Camp, S. M., Ceco, E., Evenoski, C. L., Danilov, S. M., Zhou, T., Chiang, E. T., et al. (2015). Unique toll-like receptor 4 activation by NAMPT/PBEF induces NFκB signaling and inflammatory lung injury. *Scientific Reports, 5*, 13135.

Cerna, D., Li, H., Flaherty, S., Takebe, N., Coleman, C. N., & Yoo, S. S. (2012). Inhibition of nicotinamide phosphoribosyltransferase (NAMPT) activity by small molecule GMX1778 regulates reactive oxygen species (ROS)-mediated cytotoxicity in a p53-and nicotinic acid phosphoribosyltransferase1 (NAPRT1)-dependent manner. *Journal of Biological Chemistry, 287*, 22408–22417.

Hwang, D. H., Kim, J., & Lee, J. Y. (2016). Mechanisms for the activation of Toll-like receptor 2/4 by saturated fatty acids and inhibition by docosahexaenoic acid. *European Journal of Pharmacology, 785*, 24–35.

Ji, C. L., Jiang, H., Tao, M. Q., Wu, W. T., Jiang, J., & Zuo, J. (2017). Selective regulation of IKKβ/NF-κB pathway involved in proliferation inhibition of HFLS-RA cells induced by 1,7-dihydroxyl-3,4-dimethoxylxanthone. *Kaohsiung Journal of Medical Sciences, 33*, 486–495.

Ji, J., Wang, Q., Wang, M., Chen, J., & Li, X. (2019). New lignan glycosides from the stems of *Securidaca inappendiculata* Hassk. *Phytochemistry Letters, 31*, 58–62.

Jiang, H., Ji, C. L., Yang, K., Zhang, W., & Zuo, J. (2018). Fatty oil from *Securidaca inappendiculata* exerted therapeutic effects on adjuvant-induced arthritis in mice via suppression on fibroblast-like synoviocyte. *Kaohsiung Journal of Medical Sciences, 34*, 616–625.

Li, Y. W. (2005). *Studies on the anti-inflammatory-immune and analgesic effects and their mechanisms of WWT. Master's Dissertation*. Nanning: Guangxi University of Medicine.

Dong, L., Wang, S., Chen, M., Li, H., & Bi, W. (2008). The activation of macrophage and upregulation of CD40 costimulatory molecule in lipopolysaccharide-induced acute lung injury. *Journal of Biomedicine and Biotechnology, 2008* 852571.

Pulla, V. K., Sriram, D. S., Soni, V., Viswanadha, S., Sriram, D., & Yogeeswari, P. (2015). Targeting NAMPT for therapeutic intervention in cancer and inflammation: Structure-based drug design and biological screening. *Chemical Biology & Drug Design, 86*, 881–894.

Ryu, S., Lim, W., Bazer, F. W., & Song, G. (2017). Chrysin induces death of prostate cancer cells by inducing ROS and ER stress. *Journal of Cellular Physiology, 232*, 3786–3797.

Soni, S., Wilson, R. M., O'Dea, P. K., Yoshida, M., Katbeh, U., Woods, J. S., et al. (2016). Alveolar macrophage-derived microvesicles mediate acute lung injury. *Thorax, 71*, 1020–1029.

Tao, M., Jiang, J., Wang, L., Li, Y., Mao, Q., Dong, J., et al. (2018). α-Mangostin alleviated lipopolysaccharide induced acute lung injury in rats by suppressing NAMPT/NAD controlled inflammatory reactions. *Evidence-based Complementary and Alternative Medicine, 2018*, 5470187.

Tsikas, D. (2016). Assessment of lipid peroxidation by measuring malondialdehyde (MDA) and relatives in biological samples: Analytical and biological challenges. *Analytical Biochemistry, 524*, 13–30.

Yang, K., Yin, Q., Mao, Q., Dai, S., Wang, L., Dong, J., et al. (2019). Metabolomics analysis reveals therapeutic effects of α-mangostin on collagen induced arthritis in rats by down-regulating nicotinamide phosphoribosyltransferase. *Inflammation, 42*, 741–753.

Yang, X. (2001). *Studies on the chemical constituents and bioactivities of medicinal plant Securidaca inappendiculata Hassk. Doctoral Dissertation*. Beijing: Peking Union Medical College.

Yang, Z., Yin, Q., Olatunji, O. J., Li, Y., Pan, S., Wang, D.-D., et al. (2020). Activation of cholinergic anti-inflammatory pathway involved in therapeutic actions of α-mangostin on lipopolysaccharide induced acute lung injury in rats. *International Journal of Immunopathology and Pharmacology, 34*. https://doi.org/10.1177/2058738420954941.

Yu, M., Wang, H., Ding, A., Golenbock, D. T., Latz, E., Czura, C. J., et al. (2006). HMGB1 signals through toll-like receptor (TLR) 4 and TLR2. *Shock, 26*, 174–179.

Zhang, J., Chen, Q., Wang, S., Li, T., Xiao, Z., Lan, W., et al. (2017). α-Mangostin, a natural xanthone, induces apoptosis and ROS accumulation in human rheumatoid fibroblast-like synoviocyte MH7A cells. *Current Molecular Medicine, 17*, 375–380.

Zuo, J., Mao, K. J., Yuan, F., Li, X., & Chen, J. W. (2014a). Xanthones with anti-tumor activity isolated from *Securidaca inappendiculata*. *Medicinal Chemistry Research, 23*, 4865–4871.

Zuo, J., Xia, Y., Mao, K. J., Li, X., & Chen, J. W. (2014b). Xanthone-rich dichloromethane fraction of *Securidaca inappendiculata*, the possible antirheumatic material base with anti-inflammatory, analgesic and immunodepressive effects. *Pharmaceutical Biology, 52*, 1367–1373.

Zuo, J., Xia, Y., Li, X., & Chen, J. W. (2014c). Therapeutic effects of dichloromethane fraction of *Securidaca inappendiculata* on adjuvant-induced arthritis in rat. *Journal of Ethnopharmacology, 153*, 352–358.

Zuo, J., Xia, Y., Li, X., & Chen, J. W. (2014d). Xanthones from *Securidaca inappendiculata* exert significant therapeutic efficacy on adjuvant-induced arthritis in mice. *Inflammation, 37*, 908–916.

Zuo, J., Dou, D. Y., Wang, H. F., Zhu, Y. H., Li, Y., & Luan, J. J. (2017). Reactive oxygen species mediated NF-κB/p38 feedback loop implicated in proliferation inhibition of HFLS-RA cells induced by1,7-dihydroxy-3,4-dimethoxyxanthone. *Biomedicine & Pharmacotherapy, 94*, 1002–1009.